An Elastic Demand Model for Locating Electric Vehicle Charging Stations

Xu Ouyang[1] · **Min Xu**[1] · **Bojian Zhou**[2] ⓘD

Abstract

In this study, we aim to optimally locate multiple types of charging stations, e.g., fast-charging stations and slow-charging stations, for maximizing the covered flows under a limited budget while taking drivers' partial charging behavior and nonlinear demand elasticity into account. This problem is first formulated as a mixed-integer nonlinear programming model. Instead of generating paths and charging patterns, we develop a compact formulation to model the partial charging logic. The proposed model is then approximated and reformulated by a mixed-integer linear programming model by piecewise linear approximation. To improve the computational efficiency, we employ a refined formulation using an efficient Gray code method, which reduces the number of constraints and binary auxiliary variables in the formulation of the piecewise linear approximate function effectively. The ε-optimal solution to the proposed problem can be therefore obtained by state-of-the-art MIP solvers. Finally, a case study based on the highway network of Zhejiang Province of China is conducted to assess the model performance and analyze the impact of the budget on flow coverage and optimal station selection.

Keywords Charging station location · Partial charging · Nonlinear elastic demand · Piecewise linear approximation · Gray code

1 Introduction

Electric vehicles (EVs) have gained much attention from the public over the past decades. As a green transport mode, EVs have high energy efficiency and generate significantly fewer emissions compared to traditional transport modes such as gasoline vehicles, yielding a variety of environmental and social benefits. However, the limited

---

✉   Bojian Zhou
     zbj387@gmail.com

[1]   Department of Industrial and Systems Engineering, The Hong Kong Polytechnic University, Hung Hom, Hong Kong

[2]   School of Transportation, Southeast University, Nanjing 210096, China

driving range and scarce charging facilities hinder the wide adoption of EVs, especially for long-distance trips, during which drivers may need to charge several times to ensure the journey. In addition, steep roads, the variation of driving speed, and the use of auto electrical parts, etc. would lead to more energy consumption and thus call for more frequent charging than normal (De Cauwer et al. 2015). To promote the adoption of EVs, many governments have substantially invested in building public charging facilities. The State Power Grid of China, for example, plans to invest RMB ¥1.1 billion in the charging station construction in Zhejiang Province by the end of 2020 (XinhuaNet 2018).

There are multiple types of charging facilities in the market. These charging stations can be classified into two main types by the power rate used, i.e., fast-charging stations and slow charging stations (Morrow et al. 2008). Fast-charging stations usually use power of over 50kWh, while slow-charging stations use power of less than 20kWh. Compared with a slow-charging station, a fast-charging station offers a much higher charging efficiency but incurs larger procurement and installation cost. For example, a fast-charging station can fully charge a 60kWh battery within an hour, while a slow-charging station needs several hours to fully charge it (Yilmaz and Krein 2012). As for the construction cost, according to the report of the U.S. Energy Department, the costs of building a fast-charging station and a slow-charging station are $8.5 million and $4.25 million, respectively (NREL 2012). In light of the huge investment and characteristics of different types of charging stations, it is imperative to develop an optimization model of deploying multiple types of charging stations so as to fulfill as many charging demands as possible under a limited budget.

1.1 Literature Review

Over the past years, many studies have focused on the refueling facility location problem for EVs and other alternative fuel vehicles. Among these studies, Hodgson (1990) was the first to develop a flow capturing location model (FCLM) to cover as many flows as possible. A flow between an origin-destination(OD) pair was assumed to be covered if there was at least one refueling station along its travel path. Kuby and Lim (2005) extended the FCLM by developing a flow refueling location model (FRLM) where drivers may need to refuel the energy several times to complete a journey. Both the FCLM and FRLM assumed that drivers would travel on the shortest path between an OD pair. Kim and Kuby (2012) later put forward a deviation flow refueling location model (DFRLM) to characterize drivers' detour behavior for charging. Specifically, drivers were allowed to travel along any deviation path other than the shortest path as long as the distance of the deviation path did not exceed a pre-specified maximal acceptable distance deviation. Since then, many follow-up studies have been conducted on top of FRLM and RFRLM (Capar et al. 2013; Guo et al. 2018; He et al. 2018; Kuby and Lim 2007; Lim and Kuby 2010; Upchurch et al. 2009; Wang and Lin 2009; Xu et al. 2020; Yang et al. 2017).

All the aforementioned studies assumed that EVs would be fully charged upon a charging station. This assumption is reasonable for a battery-swapping station where a depleted battery is swapped to a fully charged one within a few minutes but may not be so for a charging station. In the real world, drivers prone to partially their vehicles at visited stations along the trip. This is because fully charging is costly and time

consuming due to the limitation of battery and charging technologies. Fully charging en route largely increases travel time and charging cost, likely leading to late arrival at destinations. Besides, waiting hours at charging stations could make drivers uncomfortable. It is more practical to utilize dwelling time at origins and destinations to fully refuel the battery. These facts have been observed by many empirical and analytical studies such as Lin and Greene (2011); Xu et al. (2017); Chen et al. (2017); Meng et al. (2019); Quirós-Tortós et al. (2018); Quirós-Tortós et al. (2015); Wang et al. (2021); Yuan et al. (2019). Although it is more realistic, to the best of our knowledge, so far, no studies have considered drivers' partial charging behavior in the deployment of charging stations. Assuming fully charging provides significant convenience for modeling. In particular, all possible travel paths feasible to deviation tolerance are pre-generated and then a path selection model subject to station deployment is established. Under the fully charging assumption, once a path is given, the total charging cost and travel time can be computed by tracking the change of SOC node by node, and the charging amount at the visited station is obtained by the criterion of fully charging. However, this is not the case for partial charging. Since we do not know the charging amount at each station, it is impractical to calculate the charging cost and charging time. On this occasion, the charging amount is a decision variable to be optimized and the location model cannot be developed via path pre-generation. This motivates us to devise a compact model to formulate partial charging behavior without resort to path and charging pattern generation.

Moreover, in the real world, travel demand is generally affected by some external factors, e.g., travel costs. Travelers may switch to other economic transport modes if traveling with EVs is costly (Souche 2010). Among the limited relevant studies, only a few studies have considered nonlinear demand elasticity in the context of refueling station location problem (e.g., Capar et al. (2013); Kim and Kuby (2012)). However, their model is based on path pre-generation. On this occasion, the property (i.e., linear or nonlinear) of the elastic demand function does not affect model solving and the resultant model is a linear MIP model. The reason is that since all feasible travel paths are pre-generated, the travel cost of a particular path is also known a prior. Therefore, the flows along a path are obtained by substituting the travel cost of that path to the elastic demand function. The flow volume of a certain path is essentially a parameter in this case. On the contrary, getting rid of the enumeration method, formulating travel cost and flow volume as decision variables under nonlinear relationship yields a nonlinear MIP model. How to solve the nonlinear MIP model effectively and efficiently deserves further investigation.

1.2 Objective and Contributions

To fill the above research gaps, we investigate the multi-type charging station location (MCSL) problem while considering path deviation, partial charging, and nonlinear elastic demand. We consider a generalized travel cost (GTC) comprised of travel time on the path, charging time and charging fee at the traversed stations. Drivers could take a deviation path other than the shortest path as long as the GTC of the deviation path is within a pre-specified tolerance, which is often referred to as path deviation in the literature. Additionally, instead of fully charging each time, drivers are allowed to charge as much as needed to make the GTC as small as possible. As for the nonlinear

elastic demand, the flows between an OD pair are assumed to decline nonlinearly with respect to the GTC. Our goal is to maximize the covered flows of all OD pairs by determining the deployment of multi-type charging stations under a limited budget. To achieve this objective, we first formulate a mixed-integer nonlinear programming model. Instead of generating paths and charging patterns, we develop a compact formulation to model the partial charging logic. The proposed model is then approximated and reformulated by a mixed-integer linear programming model by piecewise linear approximation. To improve the computational efficiency, we employ a refined formulation using Gray code method, which effectively reduces the number of constraints and binary auxiliary variables in the formulation of the piecewise linear approximate function. The ε-optimal solution[1] to the MCSL problem is finally obtained by solving the formulation using a state-of-the-art MIP solver.

In all, the contributions of this study are multidimensional. First, we make the first attempt to incorporate drivers' partial charging behavior and nonlinear elastic demand in the charging station location problem. Second, instead of path and charging pattern enumeration, a compact formulation is put forward to model the partial charging logic. Last, the nonlinearity resulting from the elastic demand is addressed by piecewise linear approximation formulated using an efficient Gray code method.

The remainder of this paper is organized as follows. The related notations, assumptions, and problem descriptions are illustrated in Section 2. A mixed-integer nonlinear programming model is formulated in Section 3. Section 4 elaborates the piecewise linear approximation with a Gray code method. A case study based on the highway network of Zhejiang Province and impact analysis of the budget are presented in Section 5. Section 6 concludes the paper with recommendations for future research directions.

2 Assumptions, Notations and Problem Description

We consider an intercity road network $\mathcal{G} = (N, A)$, where N and A are sets of nodes and directed links, respectively. The electricity consumption and travel time of link $(i, j) \in A$, $i, j \in N$ are denoted by e_{ij} and d_{ij}, respectively, which are assumed to be known in advance. All OD pairs are grouped into a set W. The origin and destination of an OD pair $w \in W$ are denoted by $o(w)$ and $d(w) \in N$, respectively. Note that the traffic flows between locations A and B are often bi-directional: one is from A to B and the other is from B to A, referred to as a round trip. Generally, to enable round trips, we can use two direction-supplementary flows of an OD pair as the model input. The EVs are assumed to be homogeneous in terms of the battery capacity, denoted by E. For an OD pair w, the state-of-charge(SOC) of EVs is assumed to be no more than E_o before departing from $o(w)$ and no less than E_D after arriving at $d(w)$, where both E_o and E_D are pre-defined. Kindly note that we can set E_O and E_D to be any value and our model is still applicable as E_O and E_D are parameters. If EVs are of different types and battery capacities, from a modeling point of view, we can introduce several types of flows between an origin and a destination. A certain type of flows between a particular OD pair corresponds to a vehicle type, battery capacity, and even SOC at origins and

---

destinations. In other words, we can augment the set of OD pairs by vehicle types, capacities, and even battery levels.

We consider locating multi-type charging stations at a set of candidate locations, denoted by $I \subseteq N$. The types of stations are denoted by set K and the cost of building type $k \in K$ station at location $i \in I$ is $b_{i,k}$. The charging efficiency and charging price of different stations vary, which will be illustrated in the following subsection. The total budget for building public charging stations is represented by B. For simplicity, we assume that the charging stations are uncapacitated and there is at most one type of station at a candidate location. The "uncapacitated" herein means that an EV can be charged upon entering a station. In other words, the drivers do not need to queue for service. With this assumption, it is reasonable to define the GTC by the sum of charging cost, charging time, and travel time. Incorporating queueing process requires other sophisticated techniques such as queueing theory. Many facility location studies thus adopt "uncapacitated" assumptions for the consideration of modeling (e.g., Capar et al. (2013); Kim and Kuby (2012); Kuby and Lim (2007); Yang and Sun (2015)). Likewise, the focal point of this research is not the modeling queueing process. Therefore, we also use this assumption.

The following subsections elaborate on the partial charging logic, the generalized travel cost, and the nonlinear elastic demand. The notations used throughout this study can be found in Appendix 1.

2.1 Partial Charging Logic

To model drivers' partial charging behavior without resorting to path and charging pattern enumeration, we need to formulate the partial charging logic explicitly. The partial charging logic refers to the locations chosen for charging and the corresponding charging amount at these stations for each OD pair. To this purpose, we define the following decision variables and auxiliary variables to specify where and how much to charge. Among these variables, we have three binary decision variables as follows: (i)$y_{i,k}$, $\forall\, i \in I, k \in K$ denoting whether type k station is built at location i; (ii)r_i^w, $\forall i \in I, w \in W$ indicating whether EVs are charged at location i for OD pair w; and (iii)x_{ij}^w, $\forall (i, j) \in A, w \in W$ representing whether link (i, j) is traversed for OD pair w. We also have a continuous decision variable p_i^w, $\forall i \in I, w \in W$ which represents the charging amount at location i for OD pair w and a continuous auxiliary variable e_i^w, $\forall i \in N, w \in W$ that expresses the vehicle SOC of flows between OD pair w after charging at location $i \in I$ (for $i \notin I$, it represents the SOC upon arriving at location i). Given these variables, drivers' partial charging behavior can be formulated as follows.

$$\sum_{j \in N:(i,j) \in A} e_{ij} x_{ij}^w \le e_i^w \le E, \quad \forall w \in W, i \in N \tag{1}$$

$$r_i^w \le \sum_{k \in K} y_{i,k}, \quad \forall w \in W, i \in I \tag{2}$$

$$p_i^w \le E r_i^w, \quad \forall w \in W, i \in I \tag{3}$$

$$e_j^w - p_j^w - e_i^w + e_{ij} \begin{cases} \leq M\left(1 - x_{ij}^w\right) \\ \geq M\left(x_{ij}^w - 1\right) \end{cases} \quad \forall w \in W, j \in I, i \in N : (i,j) \in A \qquad (4)$$

$$e_j^w - e_i^w + e_{ij} \begin{cases} \leq M\left(1 - x_{ij}^w\right) \\ \geq M\left(x_{ij}^w - 1\right) \end{cases} \quad \forall w \in W, j \in N \backslash I, i \in N : (i,j) \in A \qquad (5)$$

where M is a sufficiently large positive number.

It can be seen that Eq. (1) ensures the link feasibility. Eq. (2) suggests that drivers can only charge at the locations where charging stations are built. Eq. (3) indicates that the charging amount cannot exceed the battery capacity if any. Equation (4) establishes the SOC relationship between a candidate location and its adjacent locations. Specifically, if link (i, j) is traversed for OD pair w, i.e., $x_{ij}^w = 1$, then Eq. (4) reduces to $e_j^w - p_j^w = e_i^w - e_{ij}$, where the left-hand-side(LHS) represents the SOC before charging at location j and the right-hand-side(RHS) expresses the SOC upon arriving at location j. The LHS and the RHS are equivalent in essence. As for the case of $x_{ij}^w = 0$, Eq. (4) becomes redundant. Likewise, Eq. (5) works for the locations that are not candidate locations, i.e., $N\backslash I$.

2.2 Generalized Travel Cost

Without loss of generality, we consider a generalized travel cost (GTC) comprised of three components, i.e., travel time on the path, charging time and charging fee at the traversed stations. Drivers are assumed to have a pre-specified value of time (VOT), denoted by ν. The cost converted from the travel time on the path for OD pair w using the VOT can be represented as follows:

$$d^w = \sum_{i \in N} \sum_{j \in N : (i,j) \in A} \nu d_{ij} x_{ij}^w, \quad \forall w \in W \qquad (6)$$

As for the cost resulting from charging activities, we consider both a fixed charging cost and a variable cost. Specifically, for station type k and charging amount p, the cost incurred by charging can be represented by $c_k + \mu_k p$, where c_k is the fixed cost of charging at type k station and μ_k is the charging-amount-dependent cost of charging at type k station per unit amount of charging. The cost incurred by charging over the entire trip for OD pair w can be represented by charging locations, charging amount, and station type as follows:

$$c^w = \sum_{i \in I} \sum_{k \in K} y_{i,k}\left(c_k r_i^w + \mu_k p_i^w\right), \quad \forall w \in W \qquad (7)$$

Based on the above descriptions, the GTC of OD pair w will become

$$t^w = d^w + c^w, \quad \forall w \in W \tag{8}$$

2.3 Path Deviation and Nonlinear Elastic Demand

The drivers of an OD pair are assumed to have a pre-specified tolerance for the path cost deviation. In other words, only the paths whose cost deviation from the GTC of the shortest path between that OD pair is within the tolerance can be chosen by the drivers. For OD pair w, let T^w denote the GTC of the shortest path in the network and let δ^w represent drivers' tolerance for path cost deviation. The GTC of a feasible path cannot exceed $(1 + \delta^w)T^w$. In addition, we also consider drivers' demand elasticity by assuming that the flows between an OD pair decline nonlinearly with respect to the GTC. In the spirit of the inverse distance function proposed by Kim and Kuby (2012) to describe demand elasticity in the context of refueling station location problems, we employ an inverse cost function in this study. Specifically, the nonlinear elastic demand function for OD pair w takes the following form:

$$f^w(t^w) = F^w e^{-\theta^w(t^w - T^w)}, \quad \forall w \in W, t^w \in [T^w, (1 + \delta^w)T^w] \tag{9}$$

where F^w is the flow volume when the GTC equals T^w, i.e., the maximum flow volume. If travelers need to pay more than the minimum GTC to complete trips, the flow volume will decrease. The minimum GTC is defined as below. First, we site fast-charging stations at all candidate locations. Then, we compute the GTC of each OD pair under such generous charging resources. Since the GTC cannot be further reduced by providing more charging resources, we define the resultant GTC in this setting as the minimum GTC. The parameter θ^w indicates the degree of drivers' demand elasticity, and a large value of θ^w implies that the flow volume decreases fast as the GTC increases. Both F^w and θ^w can be obtained by an empirical or analytical analysis of historical data. Figure 1 illustrates the proposed nonlinear elastic demand function, in which the flow volume declines nonlinearly with respect to the GTC.

In operations management (e.g., Wang et al. (2004) and Whitin (1955)) and marketing science (e.g., Noble and Gruca (1999) and Soysal and Krishnamurthi (2012)), it is prevalent to model customers' purchasing willingness and product prices by a nonlinear function, referred to as nonlinear elastic demand. It captures the variation of customers' demand regarding the change of costs. In the context of facility location problems, the number of travelers willing to use EVs is "demand" and the GTC is "cost". Consequently, it is assumed that the flows between an OD pair are assumed to decline nonlinearly with respect to the GTC". In fact, this assumption – nonlinear elastic demand – has been adopted by many studies on transportation in various problems (e.g., Cantarella (1997), Yang (1997), and Yang and Meng (1998)).

The objective of the MCSL problem is to deploy multiple types of public charging stations in an intercity road network under a limited budget so that (i) the flows between each OD pair travel on a path satisfying $t^w \leq (1 + \delta^w)T^w$ if any; (ii) the flow volume of an OD pair follows the nonlinear elastic demand function with respect to the GTC; and (iii) the covered flow volume of all OD pairs is maximized. Given that the objective is
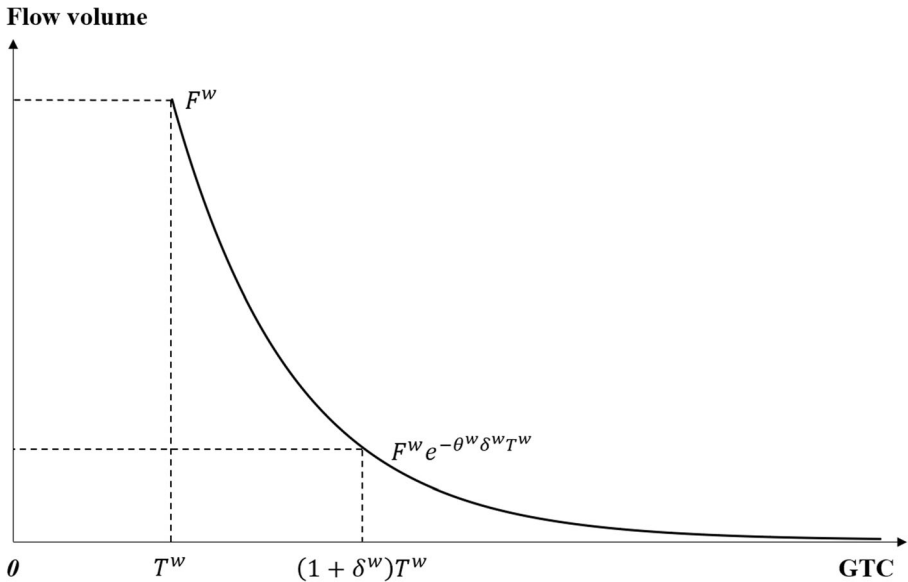
Flow volume

Fig. 1   Illustration of the nonlinear elastic demand function

to maximize the covered flows, for a particular layout of charging stations, the optimality of the model implies that drivers will travel on a range-feasible path with the minimal GTC among all feasible deviation paths, which aligns with the travel behavior of drivers.

3 Optimization Model Building

3.1 Model Formulation

In view of the situation in which some OD pairs may be uncovered due to the limited budget and driving range, we introduce a binary auxiliary variable π^w, $\forall\, w \in W$ to represent whether OD pair w is covered. The MCSL problem can be formulated by the following model:

[OP · I]:

$$\max \text{Demand}^{\text{I}} = \sum_{w \in W} f^w(t^w)\pi^w \tag{10}$$

subject to Eqs. (1)–(9) and

$$\sum_{i \in I} \sum_{k \in K} b_{i,k} y_{i,k} \leq B \tag{11}$$

$$\sum_{k \in K} y_{i,k} \leq 1, \quad \forall i \in I \tag{12}$$

$$\sum_{j\in N:(i,j)\in A}x_{ij}^w-\sum_{j\in N:(j,i)\in A}x_{ji}^w = \begin{cases} \pi^w, & \forall i = o(w) \\ 0, & \forall i\in N\setminus\{o(w),d(w)\} \\ -\pi^w, & \forall i = d(w) \end{cases} \quad \forall w\in W \quad (13)$$

$$e_{o(w)}^w \leq E_o, \quad \forall w\in W : o(w)\notin I \tag{14}$$

$$e_{o(w)}^w - p_{o(w)}^w \leq E_o, \quad \forall w\in W : o(w)\in I \tag{15}$$

$$e_{d(w)}^w \geq E_D\pi^w, \quad \forall w\in W \tag{16}$$

$$e_{d(w)}^w \geq E_D\pi^w, \quad \forall w\in W \tag{17}$$

$$x_{ij}^w, \pi^w\in\{0,1\}, \quad \forall w\in W, i,j\in N : (i,j)\in A \tag{18}$$

$$y_{i,k}, r_i^w \in \{0,1\}, \quad \forall w\in W, i\in I, k\in K \tag{19}$$

$$p_i^w, e_j^w, t^w \in \mathbb{R}_+, \quad \forall w\in W, i\in I, j\in N \tag{20}$$

where $\mathbb{R}_+$ denotes the set of non-negative real numbers.

The objective function shown by Eq. (10) represents the total covered flow volume of all OD pairs. Constraint (11) restricts that the total cost of building charging stations cannot exceed the pre-defined budget. Constraint (12) indicates that at most one type of station will be built at a candidate location. Constraint (13) is for flow conservation. Constraints (14)–(16) require that the SOC is no more than E_o before departure and no less than E_D after arrival. Note that if the origin of an OD pair is a candidate location, i.e., $o(w) \in I$, the SOC may be replenished by the amount of $p_{o(w)}^w$ as shown in Constraint (15). Constraint (17) indicates drivers' tolerance for path cost deviation. Constraints (18)–(20) specify the domains of decision variables x_{ij}^w, $y_{i,k}$, r_i^w, p_i^w and auxiliary variables π^w, e_i^w, t^w.

3.2 Model Properties

The proposed formulation for drivers' partial charging behavior explicitly models the charging location choices and charging amount without resorting to path and charging pattern enumeration. Furthermore, it is linear and has a polynomial number of

constraints. Specifically, the number of constraints in the formulation is fixed given a network. It overcomes the prohibitively large memory consumption as reported by Kim and Kuby (2012), which resulted from the exponential growth of constraints with respect to drivers' tolerance and EV driving range.

The model [OP · I] is nonlinear due to the nonlinear objective function and the bilinear terms in Eq. (7). Fortunately, the bilinear terms can be easily linearized by introducing two kinds of continuous proxy variables ($c^1_{w,i,k} = \mu_k p^w_i y_{i,k}$ and $c^2_{w,i,k} = c_k r^w_i y_{i,k}$, $\forall w \in W, i \in I, k \in K$) and imposing the following linear constraints:

$$c^w = \sum_{i \in I} \sum_{k \in K} c^1_{w,i,k} + c^2_{w,i,k}, \quad \forall w \in W \tag{21}$$

$$\begin{cases} c^1_{w,i,k} \geq 0 \\ c^1_{w,i,k} \leq \mu_k E y_{i,k} \\ c^1_{w,i,k} \geq \mu_k p^w_i + \mu_k E (y_{i,k} - 1) \\ c^1_{w,i,k} \leq \mu_k p^w_i \end{cases} \quad \forall w \in W, i \in I, k \in K \tag{22}$$

$$\begin{cases} c^2_{w,i,k} \geq 0 \\ c^2_{w,i,k} \leq c_k y_{i,k} \\ c^2_{w,i,k} \geq c_k (r^w_i + y_{i,k} - 1) \\ c^2_{w,i,k} \leq c_k r^w_i \end{cases} \quad \forall w \in W, i \in I, k \in K \tag{23}$$

We shall then show that the approximation of the bilinear terms is also exact at the boundaries. The term $c^1_{w,i,k} = \mu_k p^w_i y_{i,k}$ contains a continuous variable p^w_i and a binary variable $y_{i,k}$. If $y_{i,k} = 0$, then $c^1_{w,i,k} = 0$. In this case, Eq. (22) becomes

$$\begin{cases} c^1_{w,i,k} \geq 0 \\ c^1_{w,i,k} \leq 0 \\ c^1_{w,i,k} \geq \mu_k p^w_i - \mu_k E \\ c^1_{w,i,k} \leq \mu_k p^w_i \end{cases}$$

which indicates $c^1_{w,i,k} = 0$. If $y_{i,k} = 1$, then $c^1_{w,i,k} = \mu_k p^w_i$. On this occasion, Eq. (22) is

$$\begin{cases} c^1_{w,i,k} \geq 0 \\ c^1_{w,i,k} \leq \mu_k E \\ c^1_{w,i,k} \geq \mu_k p^w_i \\ c^1_{w,i,k} \leq \mu_k p^w_i \end{cases}$$

which implies that $c^1_{w,i,k} = \mu_k p^w_i$. Clearly, Eq. (22) is identical to $c^1_{w,i,k} = \mu_k p^w_i y_{i,k}$. With a similar approach, we can prove Eq. (23) is equivalent to $c^2_{w,i,k} = c_k r^w_i y_{i,k}$. Particularly, when $y_{i,k} = 0$, we have

$$
\begin{cases}
c^2_{w,i,k} \geq 0 \\
c^2_{w,i,k} \leq 0 \\
c^2_{w,i,k} \geq c_k \left(r^w_i - 1 \right) \\
c^2_{w,i,k} \leq c_k r^w_i
\end{cases}
$$

suggesting $c^2_{w,i,k} = 0$; when $y_{i,k} = 1$, we have

$$
\begin{cases}
c^2_{w,i,k} \geq 0 \\
c^2_{w,i,k} \leq c_k \\
c^2_{w,i,k} \geq c_k r^w_i \\
c^2_{w,i,k} \leq c_k r^w_i
\end{cases}
$$

which means $c^2_{w,i,k} = c_k r^w_i$.

As for the nonlinear objective function, we will employ a piecewise linear approximation method to address its nonlinearity, which will be elaborated in the next section.

4 Solution Approach

In this section, we employ a piecewise linear approximation method to address the nonlinearity in the objective function of the model [OP · I]. A Gray code method is employed to establish the approximation function. Compared with the traditional piecewise linear formulation to approximate nonlinear function, the Gray code method uses significantly fewer binary auxiliary variables and constraints, thereby improving computational efficiency.

4.1 Piecewise Linear Approximation

Piecewise linear approximation is a classic solution approach to nonlinear optimization problems, which has been applied in many transportation problems (Daganzo and Laval 2005; Ekström et al. 2012; Farhi 2012; Przybyla et al. 2015). In particular, a univariate continuous function can be approximated by a piecewise linear function with the approximation error being controlled by the number of linear segments (Wolsey and Nemhauser 1999). For instance, we consider the nonlinear elastic demand function for OD pair w, i.e., $f^w(t^w)$, $t^w \in [T^w, (1 + \delta^w)T^w]$, which is to be approximated by a piecewise linear function $\tilde{f}^w(t^w)$ as shown in Fig. 2. To this end, we need to first generate $V(w)$ breakpoints, denoted by t^w_n, $n = 1, \ldots, V(w)$, based on the required solution quality to specify the piecewise linear function $\tilde{f}^w(t^w)$ (see Subsection 4.2). The flow volumes corresponding to each breakpoint are $f^w(t^w_n)$, $n = 1, \ldots, V(w)$. Then it follows that any $t^w \in [T^w, (1 + \delta^w)T^w]$ can be represented by
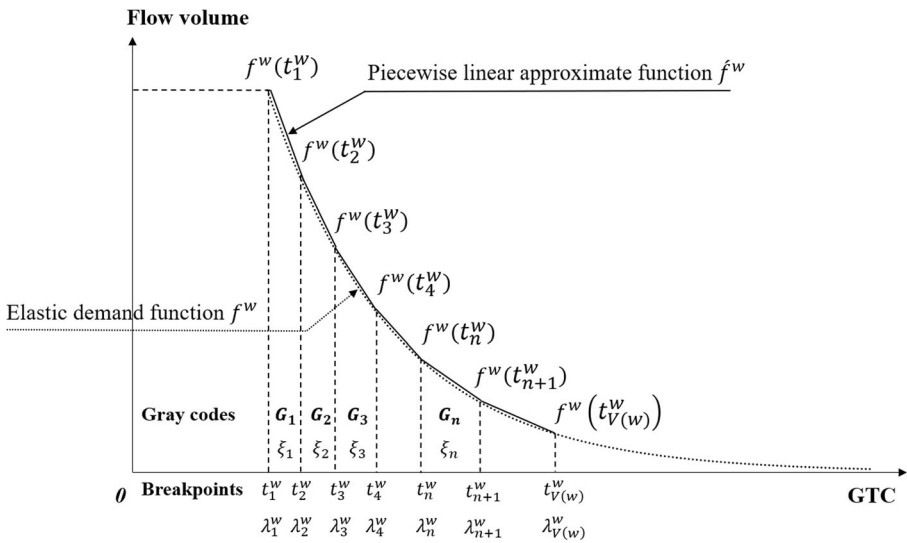
Fig. 2 Illustration of the piecewise linear approximate function

$$t^w = \sum_{n=1}^{V(w)} \lambda_n^w t_n^w \tag{24}$$

$$\sum_{n=1}^{V(w)} \lambda_n^w = 1 \tag{25}$$

$$\lambda_n^w \in \mathbb{R}_+, \quad n = 1, \ldots, V(w) \tag{26}$$

Notice that in Eqs. (24)–(26) the values of λ_n^w are not unique. However, if we have $t^w \in [t_n^w, t_{n+1}^w]$ and λ_n^w such that $t^w = \lambda_n^w t_n^w + \lambda_{n+1}^w t_{n+1}^w$ and $\lambda_n^w + \lambda_{n+1}^w = 1$, then it follows that $f^w(t^w) = \lambda_n^w f^w(t_n^w) + \lambda_{n+1}^w f^w(t_{n+1}^w)$. In other words,

$$f^w(t^w) = \sum_{n=1}^{V(w)} \lambda_n^w f^w(t_n^w) \tag{27}$$

if at most two of λ_n^w are positive and if two of λ_n^w are positive, they must be adjacent. This condition is referred to as SOS2 condition in the literature. The SOS2 condition is often formulated by introducing the binary auxiliary variables ξ_n, $n = 1, \ldots, V(w) - 1$ (where ξ_n equals 1 if $t^w \in [t_n^w, t_{n+1}^w]$ and 0 otherwise) as shown in Fig. 2 and imposing the following constraints:

$$\lambda_1^w \leq \xi_1 \tag{28}$$

$$\lambda_n^w \leq \xi_{n-1} + \xi_n, \quad n = 2, \ldots, V(w) - 1 \tag{29}$$

$$\lambda^w_{V(w)} \leq \xi_{V(w)-1} \tag{30}$$

$$\sum_{n=1}^{V(w)-1} \xi_n = 1 \tag{31}$$

$$\xi_n \in \{0, 1\}, \quad n = 1, \dots, V(w)-1 \tag{32}$$

Although the piecewise linear approximation is easy to apply to various nonlinear problems, its low computational efficiency is widely criticized due to introducing too many additional binary auxiliary variables and constraints in the formulation of SOS2 condition. Specifically, if we use $V(w)$ breakpoints to specify a piecewise linear approximate function, then $V(w) - 1$ binary auxiliary variables and $V(w) + 1$ constraints are required to formulate SOS2 condition. Many studies have been conducted to find more efficient reformulation of SOS2 condition, among which the Gray code method is very promising. The Gray-code method was developed by Vielma and Nemhauser (2011). It approximates nonlinear functions with significantly fewer auxiliary binary variables and constraints in comparison with the classic formulation of piecewise linear approximation. In fact, their reformulation of SOS2 condition using Gray code method requires only $\lceil \log_2(V(w) - 1) \rceil$ binary auxiliary variables and $2\lceil \log_2(V(w) - 1) \rceil$ linear constraints. Thus, we will employ the Gray code method to address the nonlinearity of the objective function.

To reformulate SOS2 condition by Gray code method, we need to introduce a type of special parameters, i.e., Gray code. It is a class of specially ordered multi-digit vectors with binary elements such that any two adjacent Gray codes differ in only one digit. Figure 3 illustrates Gray codes with a different number of digits, e.g., 4 two-digit Gray codes and 16 four-digit Gray codes. It can be seen that any adjacent Gray codes, e.g., the eighth four-digit Gray code {0, 1, 0, 0}. and the ninth four-digit Gray code {1, 1, 0, 0}, only differ in one digit.

To apply the Gray code method, the feasible path cost range of OD pair w, i.e., $[T^w, (1 + \delta^w)T^w]$, is first partitioned into $V(w) - 1$ intervals by $V(w)$ pre-generated breakpoints. Each interval is then labeled by a Gray code in sequence. Therefore, we need a total of $V(w) - 1$ Gray codes. To have such number of Gray codes, we need to generate these Gray codes with at least $\lceil \log_2(V(w) - 1) \rceil$ digits. Let G_n, $n = 1, \dots, V(w) - 1$ denote the sequential Gray codes with $\lceil \log_2(V(w) - 1) \rceil$ digits that we generated. For the nth interval, which is specified by the breakpoints t^w_n and t^w_{n+1}, this interval is labeled by the Gray code G_n as shown in Fig. 2.

To reformulate SOS2 condition using the Gray code method, we need to further introduce a binary auxiliary variable ξ^w_z and two sets $H^+(z, w)$ and $H^-(z, w)$ for each OD pair and each digit, i.e., $\forall w \in W, z = 1, \dots, \lceil \log_2(V(w) - 1) \rceil$, which are defined as follows:

$$H^+(z, w) = \left\{ n = 1, \dots, V(w) \middle| \begin{array}{c} \left(n = 1 \wedge G^w_{2,z} = 1 \right) \cup \left(G^w_{n-1,z} = 1 \wedge G^w_{n,z} = 1 \right) \\ \cup \left(n = V(w) \wedge G^w_{V(w)-1,z} = 1 \right) \end{array} \right\}, \tag{33}$$
$$\forall w \in W, z = 1, \dots, \lceil \log_2(V(w)-1) \rceil$$

Gray codes					
No.	Digit 4	Digit 3	Digit 2	Digit 1	
1	0	0	0	0	2 one-digit codes
2	0	0	0	1	
3	0	0	1	1	4 two-digit codes
4	0	0	1	0	
5	0	1	1	0	8 three-digit codes
6	0	1	1	1	
7	0	1	0	1	
8	0	1	0	0	
9	1	1	0	0	16 four-digit codes
10	1	1	0	1	
11	1	1	1	1	
12	1	1	1	0	
13	1	0	1	0	
14	1	0	1	1	
15	1	0	0	1	
16	1	0	0	0	

Fig. 3 Example of Gray codes

$$H^-(z,w) = \left\{ n = 1,\ldots,V(w) \middle| \begin{array}{c} \left(n = 1 \wedge G_{2,z}^w = 0\right) \cup \left(G_{n-1,z}^w = 0 \wedge G_{n,z}^w = 0\right) \\ \cup \left(n = V(w) \wedge G_{V(w)-1,z}^w = 0\right) \end{array} \right\} \quad (34)$$
$$\forall w \in W, z = 1, \ldots, \lceil \log_2(V(w)-1) \rceil$$

where $G_{n,z}^w$ denotes the value of the zth digit of the nth Gray code for OD pair w. Then SOS2 condition can be enforced by the following inequalities:

$$\sum_{n \in H^+(z,w)} \lambda_n^w \leq \xi_z^w, \quad \forall w \in W, z = 1, \ldots, \lceil \log_2(V(w)-1) \rceil \quad (35)$$

$$\sum_{n \in H^-(z,w)} \lambda_n^w \leq 1 - \xi_z^w, \quad \forall w \in W, z = 1, \ldots, \lceil \log_2(V(w)-1) \rceil \quad (36)$$

$$\xi_z^w \in \{0,1\}, \quad \forall w \in W, z = 1, \ldots, \lceil \log_2(V(w)-1) \rceil \quad (37)$$

Hereafter, we use a sample example to illustrate the Gray code method. Suppose we use 10 pre-generated breakpoints to specify a piecewise linear approximate function, the feasible path cost range is first partitioned into 9 intervals and each interval is then labeled by a Gray code. Therefore, we need at least 4 digits for these 9 Gray codes. The

generation of Gray code is a recursive procedure. To generate the four-digit Gray codes, we need to first generate all three-digit Gray codes. Specifically, given the two-digit Gray codes {0, 0}, {0, 1}, {1, 1}, and {1, 0} as shown in Fig. 3, the first 4 three-digit Gray codes can be obtained by adding "0" to the heads of {0, 0}, {0, 1}, {1, 1}, and {1, 0}, i.e., {0, 0, 0}, {0, 0, 1}, {0, 1, 1}, and {0, 1, 0}. By rearranging the two-digit Gray codes in inverse order, we get {1, 0}, {1, 1}, {0, 1}, and {0, 0}. The last 4 three-digit Gray codes can be obtained by adding "1" to the heads of {1, 0}, {1, 1}, {0, 1}, and {0, 0}, i.e., {1, 1, 0}, {1, 1, 1}, {1, 0, 1}, and {1, 0, 0}. Since we use four-digit Gray codes to label the intervals, 4 binary auxiliary variables are required. According to Eqs. (33) and (34), we have $H^+(1) = \{10\}, H^-(1) = \{1, 2, 3, 4, 5, 6, 7, 8\}, H^+(2) = \{6, 7, 8, 9, 10\}, H^-(2) = \{1, 2, 3, 4\}, H^+(3) = \{4, 5, 6\}, H^-(4) = \{1, 2, 8, 9, 10\}, H^+(4) = \{3, 7\}$, and $H^-(4) = \{1, 5, 9, 10\}$. In this case, Constraints (35) and (36) can be represented by:

$$
\begin{cases}
\lambda_{10} \leq \xi_1 \\
\lambda_1 + \lambda_2 + \lambda_3 + \lambda_4 + \lambda_5 + \lambda_6 + \lambda_7 + \lambda_8 \leq 1 - \xi_1 \\
\lambda_6 + \lambda_7 + \lambda_8 + \lambda_9 + \lambda_{10} \leq \xi_2 \\
\lambda_1 + \lambda_2 + \lambda_3 + \lambda_4 \leq 1 - \xi_2 \\
\lambda_4 + \lambda_5 + \lambda_6 \leq \xi_3 \\
\lambda_1 + \lambda_2 + \lambda_8 + \lambda_9 + \lambda_{10} \leq 1 - \xi_3 \\
\lambda_3 + \lambda_7 \leq \xi_4 \\
\lambda_1 + \lambda_5 + \lambda_9 + \lambda_{10} \leq 1 - \xi_4
\end{cases}
\tag{38}
$$

Based on the above discussions, the model [OP · I] can be approximated and reformulated by the piecewise linear approximation using the reformulation of SOS2 condition as follows:

[OP · II]:

$$
\max \mathrm{Demand}^{\mathrm{II}} = \sum_{w \in W} f^w
\tag{39}
$$

subject to Eqs. (1)–(6), (8), (9), (11)–(23), (33)–(36), and

$$
f^w = \sum_{n=1}^{V(w)} \lambda_n^w f^w(t_n^w), \quad \forall w \in W
\tag{40}
$$

$$
t^w = \sum_{n=1}^{V(w)} \lambda_n^w t_n^w, \quad \forall w \in W
\tag{41}
$$

$$
\sum_{n=1}^{V(w)} \lambda_n^w \leq \pi^w, \quad \forall w \in W
\tag{42}
$$

$$
\lambda_n^w \in \mathbb{R}_+, \xi_z^w \in \{0, 1\}, \quad \forall w \in W, n = 1, \ldots, V(w), z = 1, \ldots, \lceil \log_2(V(w) - 1) \rceil
\tag{43}
$$

The objective function shown by Eq. (39) represents the approximate covered flow volume of all OD pairs. Constraints (40)–(42) follow the traditional formulation of the piecewise linear approximation except that the sum of λ_n^w is upper bounded by π^w as shown in Eq. (42). The domains of variables λ_n^w and ξ_z^w are defined by Constraint (43).

It can be seen that the model [OP · II] is a mixed-integer linear programming model and therefore, can be readily solved by state-of-the-art MIP solvers like CPLEX. In the following subsection, we will elaborate on how to generate the breakpoints based on the required solution quality.

4.2 Breakpoint Generation

In the aforementioned approximation method, a piecewise linear curve overestimating the covered flow volume is generated for each OD pair. In theory, with sufficiently many breakpoints, the approximate curve will be very close to the objective function curve and the error can be controlled as small as possible. However, this will result in more linear segments and more variables in the expression of SOS2 condition, and in turn an over enlarged model that is computationally intensive. To balance the computational efficiency and solution quality, in this subsection, we illustrate how to generate a reasonably sized set of breakpoints to obtain the ε-optimal solution to the problem.

The idea that underlies the generation of a reasonably sized set of breakpoints is the solution quality of the model [OP · II] can be calibrated by controlling the approximation error of each piecewise linear approximate function $f^w(t^w)$, $w \in W$, which can be summarized by the following proposition:

Proposition 1 Let Demand$^{\text{I}^*}$ and Demand$^{\text{II}^*}$ denote the optimal objective values of the models [OP · I] and [OP · II], respectively. Given a pre-defined positive tolerance ε, the ε-optimal solution to the model [OP · I] can be obtained by solving the model [OP · II], i.e.,

$$\text{Demand}^{\text{I}^*} \leq \text{Demand}^{\text{II}^*} \leq \text{Demand}^{\text{I}^*} + \varepsilon \qquad (44)$$

if the generated breakpoints satisfy

$$\varepsilon_n^w \leq \frac{\varepsilon}{|W|}, \quad \forall w \in W, n = 1, \ldots, V(w)-1 \qquad (45)$$

where ε_n^w represents the approximation error in the interval $\left[t_n^w, t_{n+1}^w \right]$ for OD pair w.

The first inequality suggests the lower bound and the upper bound on the optimal objective. In particular, it is no smaller than the optimal objective value and meanwhile is no bigger than a pre-specified error plus the optimal objective. For the lower bound, as shown in Fig. 2, it is trivial to find that the piecewise linear approximate function is above the nonlinear curve except at breakpoints. Regarding the upper bound, we note that the total approximation error is the sum of errors on all elastic demand functions. The second inequality limits the approximation error on each elastic demand function

within a given threshold. Hence, once Eq. (45) holds, we can conclude that the total approximation error is also bounded by a given threshold. We then formally prove Proposition 1 as below.

Proof Let $\overline{W}$ denote the set of covered OD pairs. Without loss of generality, we assume that for an OD pair $w \in \overline{W}$ its real GTC t^w falls into the interval specified by the breakpoints $t_{n^*}^w$ and $t_{n^*+1}^w$, i.e., $t^w \in \left[t_{n^*}^w, t_{n^*+1}^w\right]$. Then we have

$$
\begin{aligned}
\text{Demand}^{I^*} &= \sum_{w \in \overline{W}} f^w(t^w) \leq \sum_{w \in \overline{W}} f^w(t^w) = \text{Demand}^{II^*} \\
&= \sum_{w \in \overline{W}} \left(f^w(t^w) + \varepsilon_{n^*}^w\right) \leq \sum_{w \in \overline{W}} \left(f^w(t^w) + \frac{\varepsilon}{|W|}\right) \\
&= \text{Demand}^{I^*} + \frac{\left|\overline{W}\right|}{|W|} \varepsilon \leq \text{Demand}^{I^*} + \varepsilon
\end{aligned}
\tag{46}
$$

This concludes the proof. □.

To generate a certain number of breakpoints that satisfy Condition (45) we will employ an iterative procedure to search for new breakpoints one by one. Let $\mathcal{S}^w$ denote the set of breakpoints for OD pair w. First, we initialize $\mathcal{S}^w$ by adding the endpoints of the feasible path cost range, i.e., T^w and $(1 + \delta^w)T^w$, into it. Then, we search the interval that is specified by two adjacent breakpoints for a new breakpoint, which is associated with the maximum approximation error in the interval. Specifically, given interval $\left[t_n^w, t_{n+1}^w\right]$, the maximum error in this interval can be obtained by solving the following problem:

$$
\max_{t_n^w \leq t^w \leq t_{n+1}^w} f^w(t^w) - F^w e^{-\theta^w(t^w - T^w)}
\tag{47}
$$

It is easy to find that the target breakpoint is

$$
\widehat{t}_n^w = T^w - \frac{1}{\theta^w} \ln \frac{-\varpi_n^w}{F^w \theta^w}
\tag{48}
$$

and the maximum approximation error in the interval is

$$
\widehat{\varepsilon}_n^w = \left(\varpi_n^w \widehat{t}_n^w + \sigma_n^w\right) - F^w e^{-\theta^w \left(\widehat{t}_n^w - T^w\right)}
\tag{49}
$$

where ϖ_n^w and σ_n^w denote the slope and intercept of the linear function of $f^w(t^w)$ in interval $\left[t_n^w, t_{n+1}^w\right]$. If $\widehat{\varepsilon}_n^w \leq \varepsilon/|W|$, this interval is labeled as qualified and will not be examined anymore; otherwise, the point $\widehat{t}_n^w$ will be added into the set $\mathcal{S}^w$ and the interval is then divided into two parts by $\widehat{t}_n^w$, i.e., $\left[t_n^w, \widehat{t}_n^w\right]$ and $\left[\widehat{t}_n^w, t_{n+1}^w\right]$, both of which

will be examined in a similar way next. The above procedure iteratively examines all existing intervals until no new breakpoints can be found. The pseudo-code of the breakpoint generation is outlined as follows:

Algorithm 1. Pseudo-code of the breakpoint generation.

|	
1	Initialization: $\mathcal{S}^w \leftarrow \{t^L, t^R\}$; // $\mathcal{S}^w$ denotes the set of breakpoints for OD pair w; T^w and $(1 + \delta^w)T^w$ are initial values of endpoints t^L and t^R, respectively.
2	**Function** $[\mathcal{S}^w] =$ **Breakpoint** $(t^L, t^R, \mathcal{S}^w)$; // recursive function iteratively searching for breakpoints in interval $[t^L, t^R]$.
3	$[\varpi, \sigma] = \textbf{\textit{Line}}(t^L, t^R)$; // ϖ and σ are the slope and intercept of the linear function cross points $\left(t^L, F^w e^{-\theta^w(t^L - T^w)}\right)$ and $\left(t^R, F^w e^{-\theta^w(t^R - T^w)}\right)$.
4	$t^B = T^w - \frac{1}{\theta^w} \ln \frac{-\varpi}{F^w \theta^w}$; // the point corresponding to the maximum error.
5	$Error = (\varpi t^B + \sigma) - F^w e^{-\theta^w(t^B - T^w)}$; // the maximum approximation error.
6	If $Error > \varepsilon/|W|$
7	$\quad \mathcal{S}^w \leftarrow t^B$;
8	$\quad [\mathcal{S}^w] = \textbf{\textit{Breakpoint}}(t^L, t^B, \mathcal{S}^w)$;
9	$\quad [\mathcal{S}^w] = \textbf{\textit{Breakpoint}}(t^B, t^R, \mathcal{S}^w)$;
10	End if
11	End function

---

5 Case Study

In this section, a case study based on the highway network of Zhejiang Province of China is conducted to examine the applicability of the proposed model and solution approach. The impact analysis of the budget on flow coverage and optimal station selections is also performed. The model is coded in MATLAB 2019a calling IBM ILOG CPLEX 12.9 on a personal desktop with Intel Core i7 4.0 GHz CPU.

5.1 Highway Network of Zhejiang Province and Parameter Settings

As reported by XinhuaNet (2018), the State Power Grid of China plans to invest RMB ¥1.1 billion in building public charging facilities in Zhejiang Province by the end of 2020. The proposed MCSL problem is expected to provide some practical insights into deploying public charging stations for the investor. The highway network of Zhejiang Province can be represented by a graph consisting of 34 nodes and 96 directed links as shown in Fig. 4. The parameters of EVs are based on BYD-EV6, which is popular with the Chinese market. Specifically, the EV battery capacity is 60kWh and the electricity consumption rate is 0.2kWh/km (BYD 2018). According to the electricity consumption rate, the speed of 120 km/h, and link distances, we can obtain the electricity consumption and travel time of each link. Following the convention in the literature, the initial/final SOC before/after departure/arrival is set to be no bigger/smaller than half of the battery capacity, i.e., 30kWh. The reason for assuming the initial/final SOC no bigger/
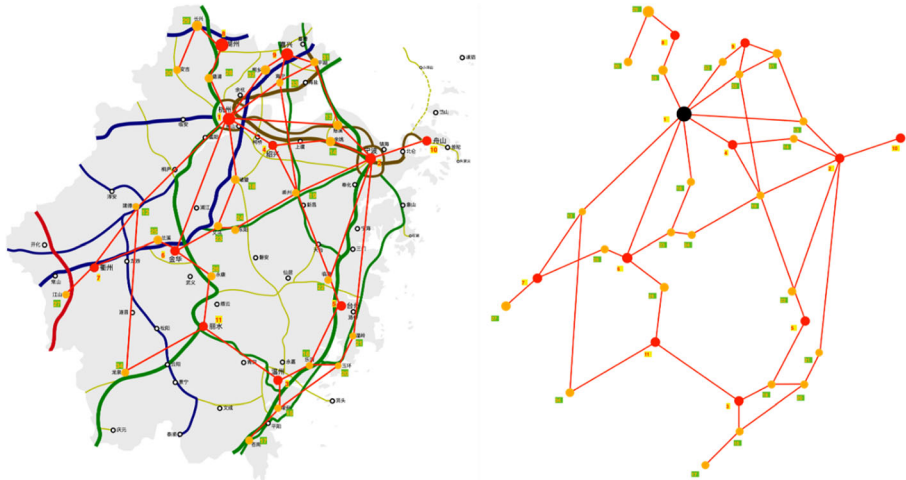
Fig. 4 Highway network of Zhejiang Province of China

smaller than 50% of battery capacity is that this SOC setting enables round trips. In particular, the drivers can travel from the destination to the origin along the same route of the inbound trip if the aforesaid SOC condition is fulfilled. Many previous studies also adopted this SOC setting to conduct numerical experiments, e.g., Kim and Kuby (2012), Kuby and Lim (2005, 2007), and Lim and Kuby (2010).

All 34 nodes in the network are candidate locations for building charging stations. The construction cost of a slow−/fast- charging station is set to be one/two unit cost for simplicity. The drivers' value of time is assumed to be $10/h. For slow−/fast- charging stations, the charging-amount-dependent cost and the fixed charging cost are $0.5/ kWh/$1.8/kWh and $1/$1, respectively The largest 20 cities (more than one million people) of Zhejiang Province are chosen as origins and destinations for generating OD pairs and then 190 OD pairs are obtained. The flow volume of each OD pair is obtained in the gravity model (Hodgson 1990) with the city population. To reduce trivial and unrealistic cases, we exclude the cases of few flows and less electricity consumption (no more than 30kWh). Finally, we remain 50 OD pairs with 23,497 flows, which account for 88.7% of total flows. As for the degree of drivers' demand elasticity θ^w, it is obtained by assuming the flow volume declines from F^w to $0.2F^w$ as the GTC rises from T^w to $1.5T^w$.

The approximation error in the piecewise linear approximation using the Gray code method is set to be 50, i.e., less than one for each OD pair. Based on this error tolerance, the required numbers of breakpoints, Gray codes, digits of Gray codes, continuous auxiliary variables, binary auxiliary variables, and linear constraints are shown by Columns 2–7 of Appendix 2. The numbers of saved binary auxiliary variables and constraints are presented by Columns 8 and 9 of Appendix 2. To analyze the impact of budget on covered flows of all OD pairs, we set the budget to be {2, 4, 6, 8, …, 28}. To further investigate the influence of drivers' tolerance for path cost deviation, the tolerance is set to be {0, 20%, 50%}. The computational time limit (elapsed time) of each instance is set to be 24 h. The experimental results of the 42 instances are displayed in Appendix 3.

5.2 Impact Analysis of Budget on Flow Coverage and Covered OD Pairs

Figures 5 and 6 present the flow coverage and the number of covered OD pairs under three tolerances as the budget varying from 2 to 28 unit cost. When the tolerance equals zero, drivers will travel on the shortest path in the network. When the tolerance becomes 20% and 50%, drivers could take a deviation path as long as the path cost deviation is within the tolerance. It can be seen that in Fig. 5 the flow coverage follows an upward trend and has a near-concave shape, suggesting that the increment rate of flow coverage decreases gradually, i.e., the marginal benefit of investment is declining. In addition, given the same budget available, the flow coverage under a high tolerance is usually bigger than that under a low tolerance. For example, given 10 unit cost, the flow coverage under zero tolerance is only 49.03%, while these numbers under 20% and 50% tolerances are 55.83% and 60.99%, respectively. From another point of view, the planner needs less investment to attain the same flow coverage if drivers accept a higher path cost deviation. For instance, if the target flow coverage is 60%, only 10 unit cost is required under 50% tolerance while 12 unit cost is required under zero tolerance. As for the number of covered OD pairs, it also embraces an upward trend but displays fluctuation. It can be seen that in Fig. 6 the fluctuation is especially obvious under 50% tolerance. Like the relationship of flow coverage under different tolerances, the number of covered OD pairs under a high tolerance is usually bigger than that under a low tolerance. Based on the above analysis, we can get some practical insights, i.e., a good understanding of drivers' tolerance for path cost deviation contributes to saving the budget or satisfying more charging demands.

5.3 Impact Analysis of Budget on Optimal Station Selection

The number of slow−/fast- charging stations as the budget rises from 2 to 28 unit cost under three tolerances is displayed by Figs. 7, 8, and 9. The number of fast-charging stations increases with respect to the budget and tends to be stable after the budget exceeds 16 unit cost. By contrast, the number of slow-charging stations fluctuates as the budget varies from 2 to 16 unit cost and then rises almost linearly after the budget goes
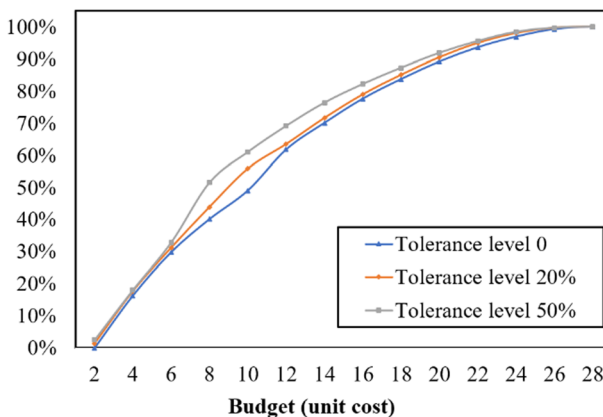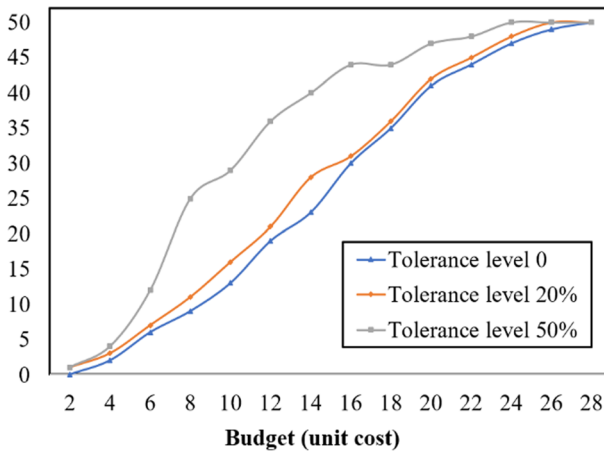

Fig. 5 Flow coverage

Fig. 6 Covered OD pairs

beyond 16 unit cost. Moreover, under three tolerances, the numbers of two types of stations go across several times, yielding many intersection points. For instance, under 20% tolerance as shown in Fig. 8, there are 3 intersection points, i.e., 6, 9, and 18 unit cost. The planner needs to locate more slow-charging stations if the budget is smaller than 9 unit cost or bigger than 18 unit cost; otherwise, more fast-charging stations should be built. In practice, the planner may prefer to build more slow-charging stations since fast-charging stations generally call for more maintenance and operation costs. Fortunately, the above results suggest that even if they need to cover all flows, only 7 fast-charging stations are required.

5.4 Impact Analysis of Driving Ranges on Flow Coverage and Station Deployment

In this section, we aim to investigate how the driving range (also battery capacity) of EVs affects the covered flow volume as well as the deployment of sited charging stations. To this end, we let the driving ranges of EVs be three values, namely 300 km,
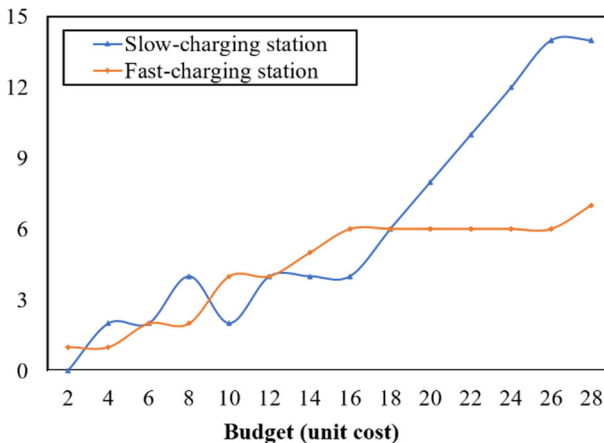

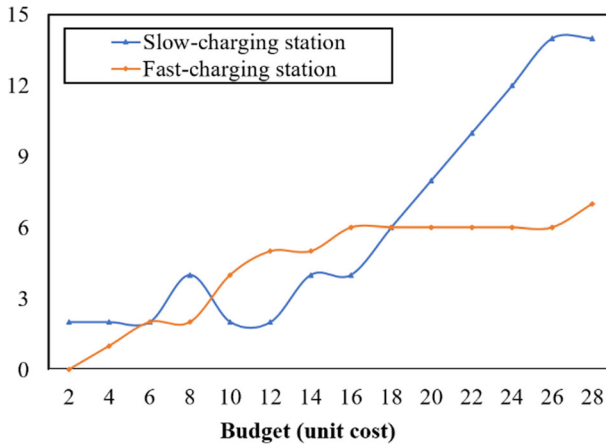Fig. 7 No. of stations under zero tolerance

Fig. 8 No. of stations under 20% tolerance

400 km, and 500 km. The drivers' tolerance for travel cost deviation is assumed to be 0.5% of their minimum GTC and we then vary the total budget from 2 unit cost to 28 unit cost (increasing 2 unit cost sequentially). To vividly showcase the impact of driving ranges on flow coverage, we visualize the experimental results under the three given ranges on the same figure as follows (P.S.: FC_D300 denotes the curve of flow coverage under the driving range of 300 km) (Figs. 10, 11, and 12).

Basically, the three curves perform a near-concave shape as the available budget increases. In particular, they all first rise stably and then tend to be a constant, i.e., 100% of flow coverage. The interesting point is that the flow coverage under a higher driving range attains 100% of flow coverage more early, that is, all travelers' charging demand is fulfilled with a smaller investment. This fact aligns with our expectation that with a longer driving range, there is no need for governments to build too many charging facilities as EVs can cruise a long distance without being replenished en route. This observation also provides valuable insights for governments into promoting
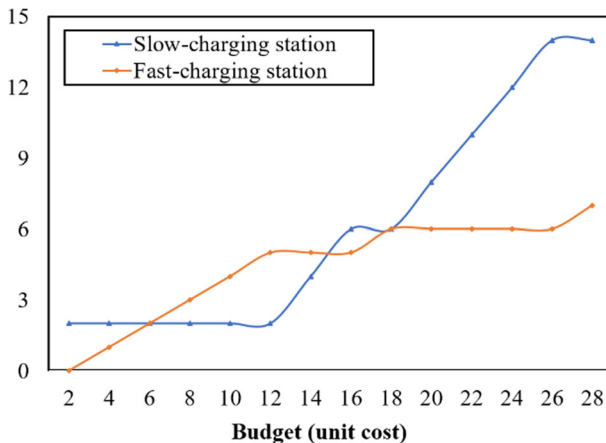

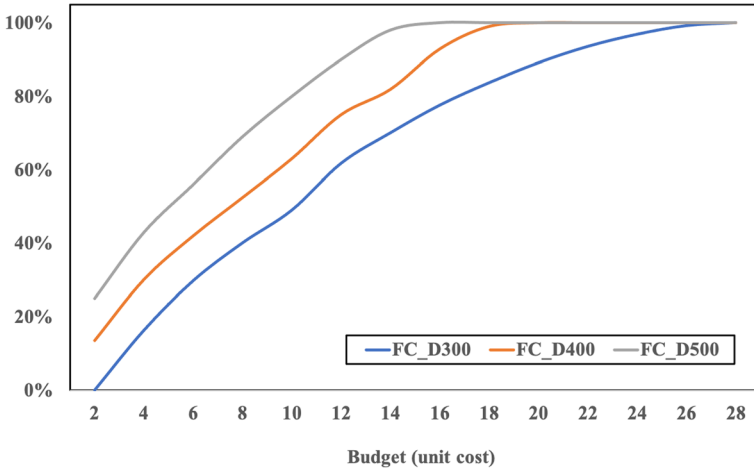**Fig. 9** No. of stations under 50% tolerance

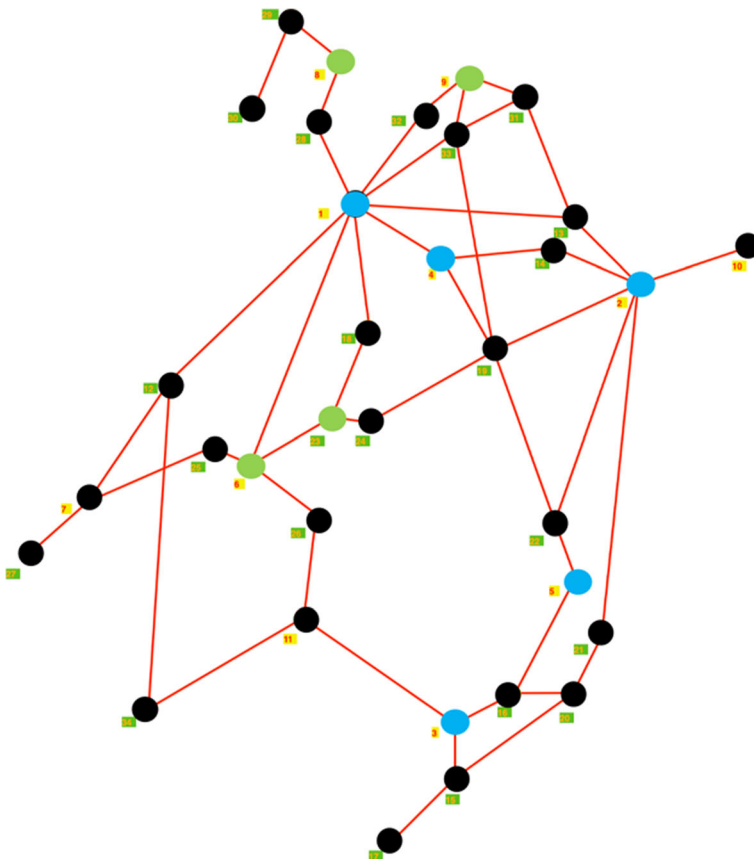**Fig. 10** Variations of flow coverage under three driving ranges as the growth of budget

Fig. 11 Station deployment under range 300 km
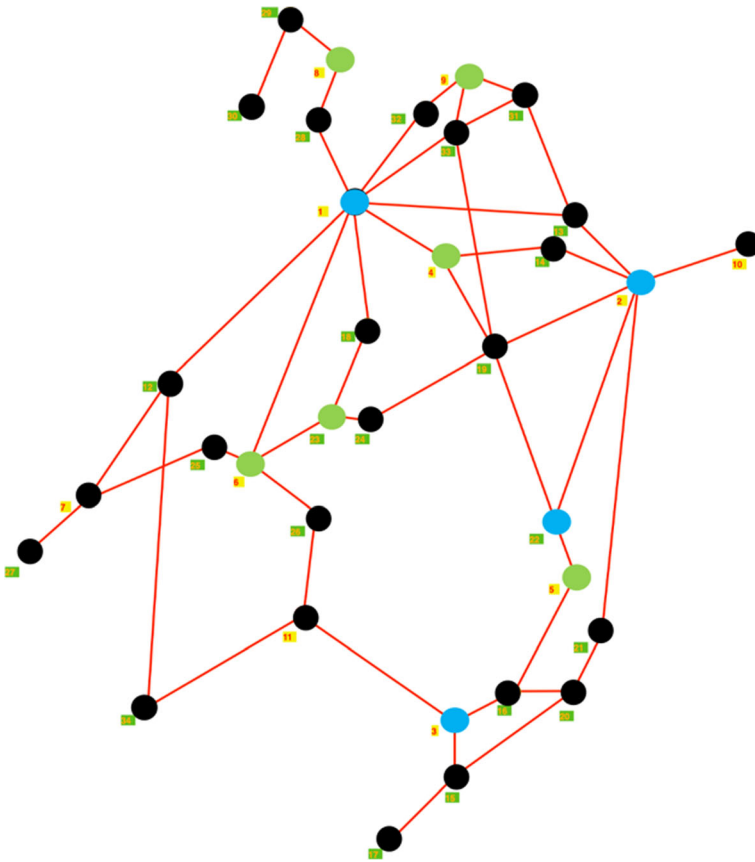
Fig. 12 Station deployment under range 400 km

green transportation. Advancing battery technologies not only boosts the development and adoption of EVs but also saves investment in building charging facilities, which is green for the environment and economy. We also present the charging station distributions under driving ranges of 300 km and 400 km and 14 unit budget below to see how stations are sited under different driving ranges.

The blue circles denote fast-charging stations; the green circles represent slow-charging stations; the black circles imply no charging stations at that node. Under the driving range of 300 km, we site five fast-charging stations at locations 1, 2, 3, 4, 5, and four slow-charging stations at locations 6, 8, 9, 23, while under the driving range of 400 km, we have four fast-charging stations located at 1, 2, 3, 22, and five slow-charging stations located at 4, 5, 6, 8, 9, 23. All locations that fast-charging stations locate are big cities of Zhejiang Province. For example, locations 1, 2, 3, 4, 5 are the biggest five cities of Zhejiang, and locations 6, 8, 9, 23 are also med-size cities. This observation coincides with our experience that fast-charging stations are generally sited in big cities. Interestingly, when a larger driving range is accessible, we only have four fast-charging stations and use the saved budget to build two additional slow-charging stations. This could attribute to that when EVs can cruise a longer distance, drivers do

not need to refuel energy multiple times and slow-charging stations are also welcome for them. This is an encouraging finding since slow-charging stations have less burden on the electricity grid and incur fewer operational costs in the long run. This finding also motivates the governments to explore more cutting-edge battery technologies.

6 Conclusions

In this study, we aim to optimally locate multi-type charging stations, e.g., fast-charging stations and slow-charging stations, for maximizing the covered flows while taking into account path deviation, partial charging, and nonlinear elastic demand. This problem is first formulated as a mixed-integer nonlinear programming model and then reformulated as a mixed-integer linear programming model by the piecewise linear approximation. In addition, a compact formulation is put forward to model the partial charging logic instead of generating paths and charging patterns. To improve the computational efficiency, we employ a refined formulation of SOS2 condition using Gray code method, which effectively reduces the number of constraints and binary auxiliary variables in the formulation of the piecewise linear approximate function. A breakpoint generation scheme is finally proposed according to the requirement of solution quality. Finally, the applicability of the proposed model and the impact of the budget on flow coverage and optimal station selections are examined based on the highway network of Zhejiang Province of China.

Future studies may be undertaken in several directions. First, the efficiency of the proposed model depends on the network size and the number of OD pairs. It is thus necessary to develop an efficient algorithm applicable to large networks. For instance, as pointed out by Vielma and Nemhauser (2011), a branch-and-cut algorithm could be developed in which the Eqs. (35) and (36) play the role of valid inequalities. Second, drivers may need to wait for charging due to limited charging spots. A queueing model can be useful to incorporate waiting costs into the present model. Last, the fear of batteries running out of power en-route, namely range anxiety, will affect drivers' charging and routing behaviors. Hence, it is worthwhile to investigate the impact of range anxiety in the future.

Appendix 1

Notation table

i, j	indices for locations
w	index for OD pair
k	index for station type
$o(w)$	index for the origin of OD pair w
$d(w)$	index for the destination of OD pair w
(i, j)	directed link from location i to location j
N	set of nodes
I	set of candidate locations for building charging stations

i, j	indices for locations
A	set of directed links
W	set of OD pairs
E	battery capacity
B	total budget
e_{ij}	electricity consumption of link (i,j)
d_{ij}	travel time on link (i,j)
E_o	SOC upper bound before departing from origins
E_D	SOC lower bound after arriving at destinations
$b_{i,k}$	cost of building type k station at location i
c_k	fixed cost of charging at type k station
μ_k	charging-amount-dependent cost per unit amount of charging at type k station
ν	drivers' value of time
F^w	maximum flow volume of OD pair w
T^w	minimum GTC of OD pair w
θ^w	degree of demand elasticity for drivers of OD pair w
δ^w	tolerance for path cost deviation for drivers of OD pair w
M	a sufficiently large positive number
x_{ij}^w	a binary decision variable which equals 1 if link (i,j) is traversed for OD pair w and 0 otherwise
$y_{i,k}$	a binary decision variable which equals 1 if type k station is built at location i and 0 otherwise
p_i^w	charging amount at location i for OD pair w
π^w	a binary auxiliary variable which equals 1 if OD pair w is covered and 0 otherwise
r_i^w	a binary auxiliary variable which equals 1 if drivers of OD pair w charge at location i and 0 otherwise
e_i^w	SOC upon arriving at location $i \in I$ or SOC after charging at $i \notin I$ for OD pair w
t^w	GTC of OD pair w
$f^w(t^w)$	piecewise linear approximate function for OD pair w
$V(w)$	number of breakpoints for OD pair w
n	index for breakpoints
t_n^w	the nth breakpoint for OD pair w
$f_n^w(t_n^w)$	flow volume corresponding to t_n^w, i.e., $F^w e^{-\theta^w(t_n^w - T^w)}$
λ_n^w	a continuous auxiliary variable associated with t_n^w
ξ_z^w	a binary auxiliary variable to reformulate SOS2 condition
$G_{n,z}^w$	value of the zth digit of the nth Gray code for OD pair w
ε	error tolerance in the piecewise linear approximation
$\mathcal{S}^w$	set of breakpoints for OD pair w
ϖ_n^w	slope of the linear function of $f^w(t_n^w)$ in interval $[t_n^w, t_{n+1}^w]$
σ_n^w	intercept of the linear function of $f^w(t_n^w)$ in interval $[t_n^w, t_{n+1}^w]$
$\hat{t}_n^w$	point corresponding to the maximum error in interval $[t_n^w, t_{n+1}^w]$
$\hat{\varepsilon}_n^w$	maximum approximation error in interval $[t_n^w, t_{n+1}^w]$

Appendix 2

Table 1 The information on the model inputs

OD	No. of BP	No. of GC	No. of DGC	No. of CAV	No. of BAV	No. of LC	No. of SBAV	No. of SC
01	29	28	5	29	5	10	24	20
02	21	20	5	21	5	10	16	12
03	15	14	4	15	4	8	11	8
04	15	14	4	15	4	8	11	8
05	13	12	4	13	4	8	9	6
06	12	11	4	12	4	8	8	5
07	12	11	4	12	4	8	8	5
08	9	8	3	9	3	6	6	4
09	9	8	3	9	3	6	6	4
10	23	22	5	23	5	10	18	14
11	19	18	5	19	5	10	14	10
12	18	17	5	18	5	10	13	9
13	16	15	4	16	4	8	12	9
14	11	10	4	11	4	8	7	4
15	11	10	4	11	4	8	7	4
16	9	8	3	9	3	6	6	4
17	9	8	3	9	3	6	6	4
18	8	7	3	8	3	6	5	3
19	8	7	3	8	3	6	5	3
20	8	7	3	8	3	6	5	3
21	8	7	3	8	3	6	5	3
22	18	17	5	18	5	10	13	9
23	13	12	4	13	4	8	9	6
24	11	10	4	11	4	8	7	4
25	10	9	4	10	4	8	6	3
26	9	8	3	9	3	6	6	4
27	8	7	3	8	3	6	5	3
28	8	7	3	8	3	6	5	3
29	8	7	3	8	3	6	5	3
30	16	15	4	16	4	8	12	9
31	14	13	4	14	4	8	10	7
32	14	13	4	14	4	8	10	7
33	13	12	4	13	4	8	9	6
34	10	9	4	10	4	8	6	3
35	9	8	3	9	3	6	6	4
36	8	7	3	8	3	6	5	3
37	8	7	3	8	3	6	5	3

Table 1 (continued)

OD	No. of BP	No. of GC	No. of DGC	No. of CAV	No. of BAV	No. of LC	No. of SBAV	No. of SC
38	8	7	3	8	3	6	5	3
39	12	11	4	12	4	8	8	5
40	11	10	4	11	4	8	7	4
41	11	10	4	11	4	8	7	4
42	10	9	4	10	4	8	6	3
43	9	8	3	9	3	6	6	4
44	8	7	3	8	3	6	5	3
45	8	7	3	8	3	6	5	3
46	7	6	3	7	3	6	4	2
47	11	10	4	11	4	8	7	4
48	9	8	3	9	3	6	6	4
49	10	9	4	10	4	8	6	3
50	8	7	3	8	3	6	5	3
Total	582	532	184	582	184	368	348	264

Abbreviations: BP (breakpoints), GC (Gray codes), DGC (digits of Gray codes), CAV (continuous auxiliary variables), BAV (binary auxiliary variables), LC (linear constraints), SBAV (saved binary auxiliary variables), and SC (saved constraints)

Appendix 3

Table 2 Experimental results

B	No Tolerance						20% Tolerance						50% Tolerance					
	CF	FC (%)	No. of COD	No. of SCS	No. of FCS	GAP (%)	CF	FC (%)	No. of COD	No. of SCS	No. of FCS	GAP (%)	CF	FC (%)	No. of COD	No. of SCS	No. of FCS	GAP (%)
2	0	0.00	0	0	1	0.00	335	1.43	1	2	0	0.00	588	2.50	1	2	0	0.38
4	3839	16.34	2	2	1	3.36	4174	17.76	3	2	1	0.00	4250	18.09	4	2	1	1.36
6	7004	29.81	6	2	2	1.64	7339	31.23	7	2	2	0.17	7721	32.86	12	2	2	1.08
8	9424	40.11	9	4	2	0.14	10,322	43.93	11	4	2	0.62	12,110	51.54	25	2	3	1.08
10	11,521	49.03	13	2	4	1.23	13,118	55.83	16	2	4	0.24	14,331	60.99	29	2	4	9.74
12	14,510	61.75	19	4	4	0.18	14,908	63.45	21	2	5	0.03	16,242	69.12	36	2	5	11.31
14	16,459	70.05	23	4	5	1.12	16,824	71.60	28	4	5	5.17	17,941	76.35	40	4	5	8.16
16	18,230	77.58	30	4	6	0.04	18,544	78.92	31	4	6	0.03	19,305	82.16	44	6	5	7.02
18	19,664	83.69	35	6	6	1.04	19,978	85.02	36	6	6	1.76	20,493	87.22	44	6	6	4.36
20	20,937	89.10	41	8	6	1.05	21,251	90.44	42	8	6	0.03	21,571	91.80	47	8	6	2.78
22	21,975	93.52	44	10	6	1.09	22,289	94.86	45	10	6	1.01	22,436	95.48	48	10	6	1.00
24	22,752	96.83	47	12	6	1.03	23,011	97.93	48	12	6	0.01	23,106	98.34	50	12	6	1.01
26	23,306	99.19	49	14	6	0.82	23,405	99.61	50	14	6	0.05	23,405	99.61	50	14	6	0.10
28	23,497	100.0	50	14	7	0.00	23,497	100.0	50	14	7	0.00	23,497	100.0	50	14	7	0.00

Abbreviations: B (budget measured by unit cost), CF (covered flows), FC (flow coverage), COD (covered OD pairs), SCS (slow-charging stations), FCS (fast-charging stations), and GAP = (best upper bound − best objective value) best objective value

References

BYD (2018) Parameters of BYD:EV6 https://www.byd.com

Cantarella GE (1997) A general fixed-point approach to multimode multi-user equilibrium assignment with elastic demand. Transp Sci 31(2):107–128

Capar I, Kuby M, Leon VJ, Tsai Y-J(2013) An arc cover–path-cover formulation and strategic analysis of alternative-fuel station locations. Eur J Oper Res 227:142–151

Chen K, Zheng F, Jiang J, Zhang W, Jiang Y, Chen K (2017) Practical failure recognition model of lithium-ion batteries based on partial charging process. Energy 138:1199–1208

Daganzo CF, Laval JA (2005) On the numerical treatment of moving bottlenecks. Transp Res Part B Methodol 39:31–46

De Cauwer C, Van Mierlo J, Coosemans T (2015) Energy consumption prediction for electric vehicles based on real-world data. Energies 8:8573–8593

Ekström J, Sumalee A, Lo HK (2012) Optimizing toll locations and levels using a mixed integer linear approximation approach. Transp Res Part B Methodol 46:834–854

Farhi N (2012) Piecewise linear car-following modeling. Transp Res Part C Emerg Technol 25:100–112

Guo F, Yang J, Lu J (2018) The battery charging station location problem: impact of users' range anxiety and distance convenience. Transp Res Part E Logist Transp Rev 114:1–18

He J, Yang H, Tang TQ, Huang HJ (2018) An optimal charging station location model with the consideration of electric vehicle's driving range. Transp Res Part C Emerg Technol 86:641–654

Hodgson, M. J. (1990). A flow-capturing location-allocation model. Geogr Anal 22(3):270–279

Kim JG, Kuby M (2012) The deviation-flow refueling location model for optimizing a network of refueling stations. Int J Hydrogen Energy 37:5406–5420

Kuby M, Lim S (2005) The flow-refueling location problem for alternative-fuel vehicles. Socio Econ Plan Sci 39:125–145

Kuby M, Lim S (2007) Location of alternative-fuel stations using the flow-refueling location model and dispersion of candidate sites on arcs. Netw Spat Econ 7:129–152

Lim S, Kuby M (2010) Heuristic algorithms for siting alternative-fuel stations using the flow-refueling location model. Eur J Oper Res 204:51–61

Lin Z, Greene DL (2011) Promoting the market for plug-in hybrid and battery electric vehicles. Transp Res Rec 2252:49–56

Meng J, Cai L, Stroe D-I, Luo G, Sui X, Teodorescu R (2019)Lithium-ion battery state-of-health estimation in electric vehicle using optimized partial charging voltage profiles. Energy 185:1054–1062

Morrow, K., Karner, D., Francfort, J., 2008. Plug-in hybrid electric vehicle charging infrastructure review final report Battelle energy Alliance contract no. 58517. US Dep. Energy-vehicle Technol. Progr. 34

Noble PM, Gruca TS (1999) Industrial pricing: theory and managerial practice. Mark Sci 18(3):435–454

NREL (2012)Plug-In electric vehicle handbook for public charging station hosts, Clean Cities Technical Response Service. https://doi.org/DOE/GO-102012-3257

Przybyla J, Taylor J, Jupe J, Zhou X (2015) Estimating risk effects of driving distraction: a dynamic errorable car-following model. Transp Res Part C Emerg Technol 50:117–129

Quirós-Tortós J, Ochoa LF, Lees B (2015) A statistical analysis of EV charging behavior in the UK, 2015 IEEE PES innovative smart grid technologies Latin America (ISGT LATAM). IEEE, pp 445–449

Quirós-Tortós J, Navarro-Espinosa A, Ochoa LF, Butler T (2018) Statistical representation of EV charging: real data analysis and applications, 2018 Power Systems Computation Conference (PSCC). IEEE, pp:1–7

Souche S (2010) Measuring the structural determinants of urban travel demand. Transp Policy 17:127–134

Soysal GP, Krishnamurthi L (2012) Demand dynamics in the seasonal goods industry: an empirical analysis. Mark Sci 31(2):293–316

Upchurch C, Kuby M, Lim S (2009) A model for location of capacitated alternative-fuel stations. Geogr Anal 41:85–106

Vielma JP, Nemhauser GL (2011) Modeling disjunctive constraints with a logarithmic number of binary variables and constraints. Math Program 128(1–2):49–72

Wang YW, Lin CC (2009) Locating road-vehicle refueling stations. Transp Res Part E Logist Transp Rev 45: 821–829

Wang Y, Jiang L, Shen Z-J(2004) Channel performance under consignment contract with revenue sharing. Manag Sci 50(1):34–47

Wang Y, Yao E, Pan L (2021) Electric vehicle drivers' charging behavior analysis considering heterogeneity and satisfaction. J Clean Prod 286:124982

Whitin TM (1955) Inventory control and price theory. Manag Sci 2(1):61–68

Wolsey LA, Nemhauser GL (1999) Integer and combinatorial optimization. John Wiley & Sons

XinhuaNet (2018) New energy vehicles popular in Zhejiang, electric vehicle ownership exceeds 100,000. https://m.xinhuanet.com/zj/2018-10/12/c_1123549955.htm

Xu M, Meng Q, Liu K, Yamamoto T (2017) Joint charging mode and location choice model for battery electric vehicle users. Transp Res Part B Methodol 103:68–86

Xu M, Yang H, Wang S (2020) Mitigate the range anxiety: siting battery charging stations for electric vehicle drivers. Transp Res Part C Emerg Technol 114:164–188

Yang H (1997) Sensitivity analysis for the elastic-demand network equilibrium problem with applications. Transp Res B Methodol 31(1):55–70

Yang H, Meng Q (1998) Departure time, route choice and congestion toll in a queuing network with elastic demand. Transp Res B Methodol 32(4):247–260

Yang J, Sun H (2015) Battery swap station location-routing problem with capacitated electric vehicles. Comput Oper Res 55:217–232

Yang J, Guo F, Zhang M (2017) Optimal planning of swapping/charging station network with customer satisfaction. Transp Res Part E Logist Transp Rev 103:174–197

Yilmaz, M., Krein, P.T. (2012) Review of charging power levels and infrastructure for plug-in electric and hybrid vehicles, 2012 IEEE international electric vehicle conference, IEVC 2012

Yuan Y, Zhang D, Miao F, Chen J, He T, Lin S (2019) p^ 2Charging: proactive partial charging for electric taxi systems, 2019 IEEE 39th International Conference on Distributed Computing Systems (ICDCS). IEEE, pp. 688-699